Slot-Coupled T-Junction of TE_{11} Coaxial to TE_{10} Rectangular Waveguide

SAAD MICHAEL SAAD, SENIOR MEMBER, IEEE

Abstract—**A solution is presented to the problem of a slot-coupled T-junction of a TE_{11}-mode coaxial to a TE_{10}-mode rectangular waveguide. A variational technique is employed which combines the reaction concept with the field representation of a waveguide slot and leads to a closed-form solution for the junction scattering matrix. Numerical examples illustrate the characteristics of such a junction in practical applications. Good agreement between theory and experiment is obtained. Design criteria and examples are presented and discussed.**

I. Introduction

THE SLOT-COUPLED T-junction of a TE_{11}-mode coaxial to a TE_{10}-mode rectangular waveguide (Fig. 1) is frequently encountered as a building block in a variety of waveguide components such as rotary joints, power dividers, diplexers, and antenna feeds. To the author's knowledge, however, the literature has not reported any analysis of such a junction. Marcuvitz reported a solution [1, sec. 6.10] for the closely related configuration of a T-junction composed of a TEM coaxial guide coupled through a small elliptical aperture to a rectangular waveguide. His solution, which is obtained by an integral equation method, is restricted to small apertures and to a coaxial size in which only the dominant mode may propagate.

The purpose of this paper is to provide an analysis of the TE_{11} coaxial to TE_{10} rectangular waveguide T-junction of Fig. 1, thus making the overall design of a complex structure that employs one or more of such junctions possible. The junction is first represented by an equivalent circuit then solved using a variational technique that combines the reaction concept [2] with the general field representation of a waveguide slot [3], [4]. A similar approach was previously used to analyze the rectangular-to-rectangular waveguide T-junction [5], [6]. The paper then proceeds to investigate the applicability of the theory by numerical examples and experimental verification. Finally, design criteria and applications are given and discussed.

II. Theoretical Analysis

A. Summary of Solution

In the T-junction of Fig. 1, a TE_{-11} mode traveling along the infinite coaxial guide and polarized in the y-direction will excite the longitudinal slot, and consequently the TE_{10} mode of the rectangular waveguide. Such coupling mechanism falls under the well-known category of H-plane (or shunt) T-junctions [1, sec. 3.2], [5]–[7] which may be represented by the approximate equivalent circuit of Fig. 2. Obviously, the scattering coefficients of the subject junction are determined if the value of the slot reactance jX is known. To find a good approximation for X, a variational procedure [2] may be followed. According to the reaction concept and the equivalence principle, one may find jX through the relations

$$jX = \frac{\langle a, a\rangle_1 + \langle a, a\rangle_2}{I^2} \tag{1}$$

$$\langle a, a\rangle_i = -\int_v \bar{H}_i \cdot \bar{M}\, dv \tag{2}$$

where

$\langle a, a\rangle_i$ self reaction in Guide i due to assumed $\bar{M}$,
I modal current discontinuity in Guide 1,
$\bar{M}$ equivalent magnetic current replacing the slot,
$\bar{H}_i$ magnetic field derived from the vector potential, (or otherwise) in Guide i excited by $\bar{M}$.

If a trial magnetic current is assumed, the slot reactance as calculated from (1) and (2) will be stationary about the correct solution.

B. Scattered Magnetic Field in the Coaxial Guide

An axial slot excites only the TE modes of the coaxial guide. The axial component of the scattered magnetic field in this case is given by [3]

$$H_{z1} = -\iint_A \bar{Y}_z \cdot \bar{M}\, da' \tag{3}$$

$$\bar{M} = \bar{E}_s \times \bar{n} = \bar{a}_z E_0 \sin k_0(L - |z|) \tag{4}$$

$$E_0 = V_s/2W \tag{5}$$

$$Y_z = \frac{1}{2}\sum_i \bar{Y}_i \bar{h}_{zi}(r, \phi) \cdot \bar{h}_{zi}(r', \phi') e^{-\Gamma_i |z - z'|} \tag{6}$$

$$Y_i = \frac{\Gamma_i}{j\eta k_0} \tag{7}$$

$$h_{zi}(r, \phi) = \frac{k_{ci}}{\Gamma_i}\psi_i(r, \phi) \tag{8}$$

where A is the slot area, $\bar{E}_s$ is the slot assumed (trial) field, $\bar{n}$ is the normal pointing out of the coaxial guide into the rectangular waveguide, and V_s is the slot voltage. Y_i and Γ_i

Manuscript received October 16, 1984; revised August 16, 1985.
The author is with the Andrew Corporation, Orland Park, IL 60462.
IEEE Log Number 8405926.

0018-9480/86/0100-0051$01.00 ©1986 IEEE

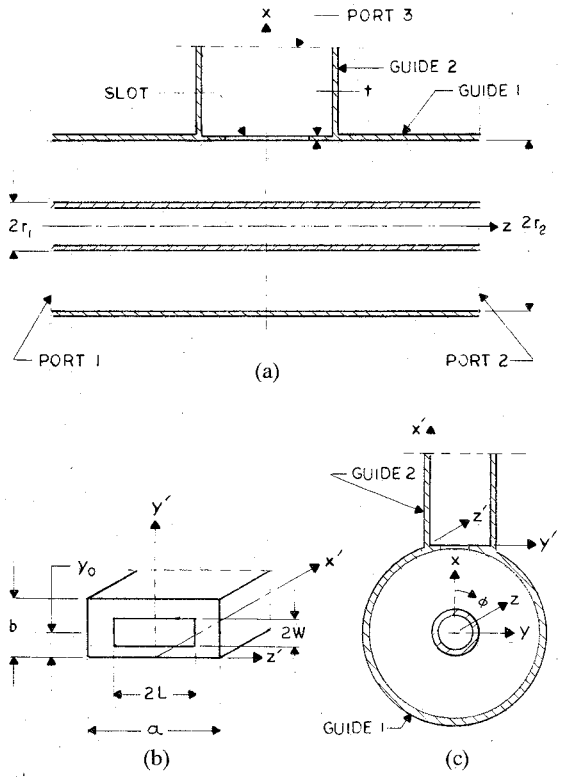

Fig. 1. Slot-coupled coaxial-to-rectangular waveguide T-junction. (a) Longitudinal section. (b) Guide 2. (c) Cross section at plane $z = 0$.

are the wave admittance and complex propagation constant of mode i. The coaxial TE_{nm} eigenfunctions ψ_i are given by [1, sec. 2.4]

$$\psi_i(r,\phi) = k_{cnm} Z_n\left(\alpha'_{nm}\frac{r}{r_1}\right)\cos n\phi \tag{9}$$

$$Z_n\left(\alpha'_{nm}\frac{r}{r_1}\right) = \frac{\sqrt{\pi\epsilon_n}\left[J_n\left(\alpha'_{nm}\frac{r}{r_1}\right)N'_n(\alpha'_{nm}) - N_n\left(\alpha'_{nm}\frac{r}{r_1}\right)J'_n(\alpha'_{nm})\right]}{2\left\{\left[\frac{J'_n(\alpha'_{nm})}{J'_n\left(\alpha'_{nm}\frac{r_2}{r_1}\right)}\right]^2\left[1-\left(\frac{n}{\alpha'_{nm}}\frac{r_1}{r_2}\right)^2\right]-\left[1-\left(\frac{n}{\alpha'_{nm}}\right)^2\right]\right\}^{1/2}},$$

$$n = 0,1,2,\cdots. \tag{10}$$

α'_{nm} is the mth root of the derivative of $Z_n(\alpha'_{nm}r_2/r_1)$, and

$$\epsilon_n = \begin{cases} 1, & n = 0 \\ 2, & n \neq 0 \end{cases} \tag{11}$$

$$\Gamma_{nm} = \sqrt{k_{cnm}^2 - k_0^2} \quad k_{cnm} = \frac{\alpha'_{nm}}{r_1} \tag{12}$$

$$\eta = \sqrt{\mu_0/\epsilon_0} = 120\pi. \tag{13}$$

In (9), the cutoff wavenumber k_{cnm} is introduced to account for the fact that [3] and [1, sec. 2.4] normalize the eigenfunctions ψ differently. Substituting from (4)–(13) in

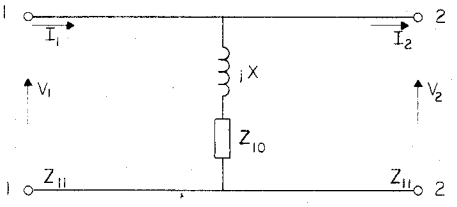

Fig. 2. Equivalent circuit of T-junction of Fig. 1.

(3) and performing the double integration

$$H_{z1}(r,\phi,z) = \sum_n\sum_m \frac{jV_s}{\eta\Gamma_{nm}} Z_n\left(\alpha'_{nm}\frac{r}{r_1}\right) \cdot Z_n\left(\alpha'_{nm}\frac{r_2}{r_1}\right)\cos n\phi \frac{\sin n\phi_0}{\frac{nW}{r_2}} \cdot\left\{\frac{\Gamma_{nm}}{k_0}\sin k_0(L-|z|) - \cos k_0 L\, e^{-\Gamma_{nm}|z|} + \cosh\Gamma_{nm} z\, e^{-\Gamma_{nm}L}\right\}, \quad -L \leqslant z \leqslant L \tag{14}$$

$$\phi_0 = \tan^{-1}\frac{W}{r_2}. \tag{15}$$

C. Self-Reaction of the Slot

Substituting from (4) and (14) into (2) and performing the integration, the slot self-reaction in the coaxial guide is obtained as follows:

$$\langle a,a\rangle_1 = \frac{j2V_s^2}{\eta}\sum_n\sum_m f_{1n}f_{1L}Z_n^2\left(\alpha'_{nm}\frac{r_2}{r_1}\right) \tag{16}$$

$$f_{1n} = \left[\frac{\sin n\phi_0}{\frac{nW}{r_2}}\right]^2 \tag{17a}$$

$$f_{1L} = \cos k_0 L\left[\sin k_0 L - \frac{k_0}{\Gamma_{nm}}\cdot\left(\cos k_0 L - 2e^{-\Gamma_{nm}L}\right)\right] - \frac{k_0}{2\Gamma_{nm}}\left(1+e^{-2\Gamma_{nm}L}\right). \tag{17b}$$

The slot self-reaction in the rectangular waveguide is given in [6] as

$$\langle a,a\rangle_2 = -\frac{j2V_s^2}{\eta}\sum_n\sum_m f_{2n}f_{2L}f_x \tag{18}$$

$$f_{2n} = \left[\frac{\sin\frac{n\pi W}{b}}{\frac{n\pi W}{b}}\right]^2 \tag{19a}$$

$$f_{2L} = \frac{k_0}{\gamma} \frac{1}{\left(\frac{m\pi}{a}\right)^2 - k_0^2} \left(\cos\frac{m\pi L}{a} - \cos k_0 L\right)^2 \tag{19b}$$

$$f_x = \begin{cases} 0, & m \text{ even} \\ \frac{2\epsilon_n}{ab} \cos^2 \frac{n\pi y_0}{b}, & m \text{ odd} \end{cases} \tag{19c}$$

$$\gamma^2 = \pi^2 \left(\frac{m^2}{a^2} + \frac{n^2}{b^2}\right) - k_0^2. \tag{19d}$$

D. Current Discontinuity in the Coaxial Guide

The presence of a lingitudinal slot in the coaxial guide gives rise to a discontinuity in the far modal currents I_1 and I_2 (Fig. 2) of the TE_{11} mode. Such current discontinuity can be related to the slot equivalent magnetic current $\bar{M}$ through transmission-line equations in the source parameter $i(z)$. Specifically, by applying [3, eqs. (3.12a) and (3.25)] to our case, we obtain

$$V_1 - V_2 = 0 \tag{20}$$

$$I_1 - I_2 \equiv I = \int_{-L}^{L} i(z') \cos\beta_{11} z'\, dz' \tag{21}$$

$$i(z) = -Y_{11} \iint_S \bar{M} \cdot \bar{h}_{z11}\, dS \tag{22}$$

where $\beta_{11} = -j\Gamma_{11}$ is defined by (12), and S is the cross section of the coaxial. Substituting from (4)–(13) in (22) then performing the integrations in (21), we obtain

$$I = \frac{j2V_s}{\eta k_{c11}} Z_1 \left(\alpha'_{11} \frac{r_2}{r_1}\right) (\cos\beta_{11} L - \cos k_0 L). \tag{23}$$

E. Equivalent Circuit Parameters

Substituting from (16)–(19) and (23) in (1), the slot reactance is finally obtained

$$X = \frac{-\eta k_{c11}^2}{2Z_1^2 \left(\alpha'_{11} \frac{r_2}{r_1}\right) (\cos\beta_{11} L - \cos k_0 L)^2} \cdot \sum_n \sum_m \left[f_{1n} f_{1L} Z_n^2 \left(\alpha'_{nm} \frac{r_2}{r_1}\right) + f_{2n} f_{2L} f_x \right] \tag{24}$$

where the different f functions are given by (17) and (19). If the wave impedances of the coaxial TE_{11} mode and the rectangular TE_{10} mode are Z_{11} and Z_{10}, respectively, then the input impedance at terminals 1-1 (Fig. 2) is

$$Z_{in} = Z_{11} \frac{Z_{10}(Z_{10} + Z_{11}) + X^2 + jXZ_{11}}{(Z_{10} + Z_{11})^2 + X^2} \tag{25}$$

$$Z_{11} = \eta k_0 / \beta_{11} \tag{26}$$

$$Z_{10} = \eta k_0 / \beta_{10}. \tag{27}$$

F. Scattering Matrix

The scattering matrix of an H-plane T-junction is represented by [7]

$$[S] = \begin{bmatrix} S_{11} & S_{12} & S_{13} \\ S_{12} & S_{11} & S_{13} \\ S_{13} & S_{13} & S_{33} \end{bmatrix}. \tag{28}$$

The four scattering coefficients in (28) may now be related to known impedances. First, S_{11} is the reflection coefficient in the coaxial guide given by

$$S_{11} = \frac{Z_{in} - Z_{11}}{Z_{in} + Z_{11}} \tag{29}$$

and if ports 2 and 3 are matched, and $P_n = P_{ni} - P_{nr}$, then

$$|S_{1n}|^2 = \frac{P_{nr}}{P_{1i}} = \frac{P_n}{P_{1i}} = \frac{P_n}{P_1}(1 - |S_{11}|^2), \qquad n = 2,3 \tag{30}$$

where P_n is the average power flowing into port n with P_{ni} and P_{nr} as its incident and reflected parts. By utilizing (25) and Fig. 2 in the relation $P_n = \frac{1}{2}\mathrm{Re}(V_n I_n^*)$, we obtain

$$P_1 = \frac{|V_1|^2}{2Z_{11}} \left[1 + \frac{Z_{10}Z_{11}}{Z_{10}^2 + X^2}\right] \tag{31}$$

$$P_2 = \frac{|V_1|^2}{2Z_{11}} \tag{32}$$

$$P_3 = \frac{|V_1|^2}{2Z_{11}} \cdot \frac{Z_{10}Z_{11}}{Z_{10}^2 + X^2}. \tag{33}$$

Substituting from (31)–(33) in (30)

$$|S_{12}|^2 = (1 - |S_{11}|^2) \frac{Z_{10}^2 + X^2}{Z_{10}^2 + X^2 + Z_{10}Z_{11}} \tag{34}$$

$$|S_{13}|^2 = |S_{12}|^2 \frac{Z_{10}Z_{11}}{Z_{10}^2 + X^2} \tag{35}$$

and applying the unitary property to the third row of $[S]$ in (28), we obtain

$$|S_{33}|^2 = 1 - 2|S_{13}|^2. \tag{36}$$

G. Slot Cross Coupling

As noted above, the present analysis is carried out for the case of a coaxial TE_{11} mode polarized parallel to the plane of the slot, i.e., polarized in the y-direction in Fig. 1. This case represents many applications where maximum slot coupling is desired. In other applications, where coupling is to be minimized, the polarization of the coaxial TE_{11} mode is chosen orthogonal to the plane of the slot. To analyze such a case, one has to employ a sine (rather than a cosine) function in (9), then carry out a derivation similar to (14)–(36). It is interesting to note that the result of such a derivation is a zero H_{z1}, $\langle a, a\rangle_1$, I, S_{11} and S_{13}, an infinite X, and a unity S_{12} and S_{33}. In physical terms, a narrow longitudinal slot is theoretically "unseen" by a coaxial TE_{11} mode polarized orthogonal to the plane of the slot.

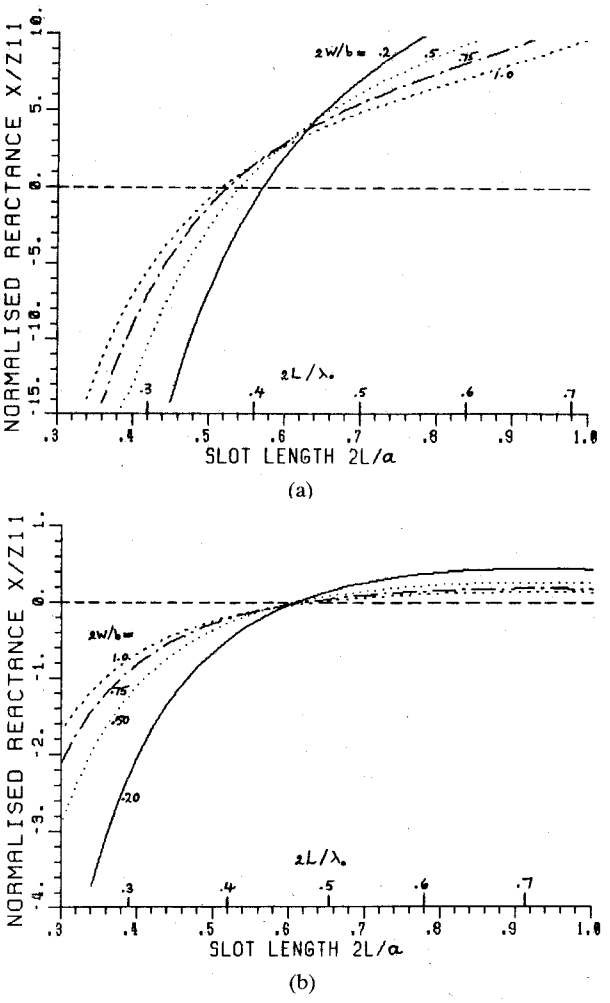

Fig. 3. Slot shunt reactance of test models. (a) 6.175-GHz signal coupled to WR137. (b) 3.95-GHz signal coupled to WR229.

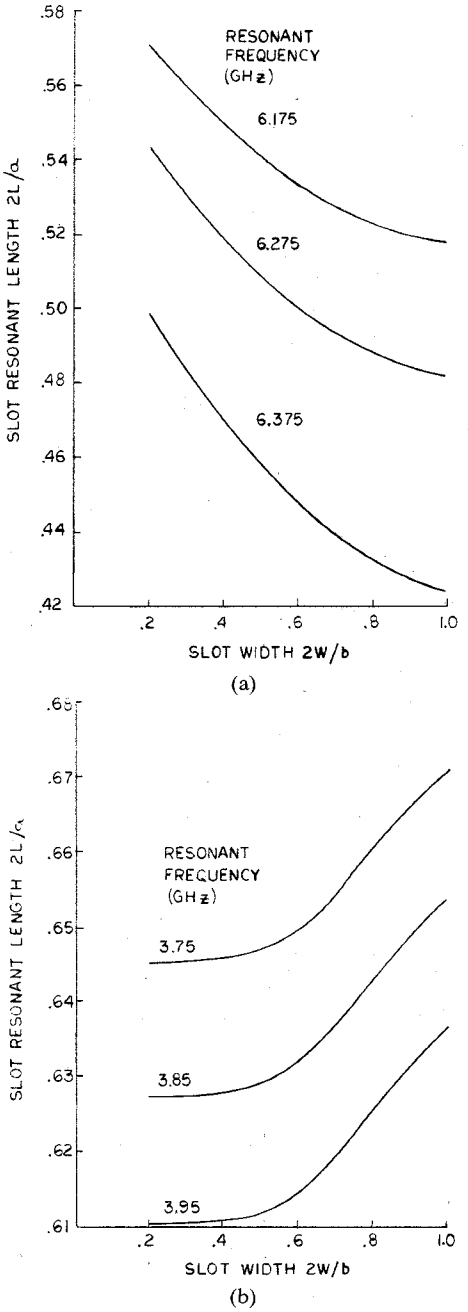

Fig. 4. Slot resonant length versus slot width for test models. (a) WR137. (b) WR229.

III. Numerical and Experimental Applications

A. Computer Program

A computer program was developed to compute the scattering coefficients. All of the theoretical expressions of Section II can be computed by a simple algorithm except the coaxial eigenfunctions $Z_n(\alpha'_{nm}r_2/r_1)$ given by (10). Accurate computation of α'_{nm} and Z_n for higher order modes requires double-precision computation of Bessel functions. The convergence of the double summation in (24) improves as the frequency increases, thus requiring fewer terms. At the lower end of the frequency band, however, still sufficient convergence is obtained for coaxial modes with $n < 20$, $m < 20$, and $n + m \leq 20$. The accuracy decreases considerably for modes with $n + m > 20$, but such modes are not usually needed. Summation over rectangular waveguide modes in (24) is much simpler and whatever accuracy is specified can be achieved.

B. T-Junction Test Models

Two test models, which represent two practical cases encountered in a multiport waveguide combiner, were examined. Such a combiner can handle copolarized signals in two or more frequency bands, each coupled from a common coaxial guide to a rectangular waveguide of suitable size. One of our T-junction test models, therefore, comprised WR137 ($a \times b = 3.485 \times 1.580$ cm), to couple the frequency band 5.925–6.425 GHz, and the other comprised WR229 ($a \times b = 5.817 \times 2.908$ cm) to couple the band 3.7–4.2 GHz. These two bands are commonly used in many microwave communication systems. Referring to Fig. 1, other dimensions of the test models are: coaxial size, $2r_1 = 14.29$ mm, $2r_2 = 43.41$ mm; slot thickness, $t = 0.56$ mm; offset, $y_0 = b/2$, $2W/b = 0.2$, and $2L/a = 0.5, 0.7$.

C. Numerical Results

Theoretical curves describing the characteristics of the test models were computed. Fig. 3 shows the variation of

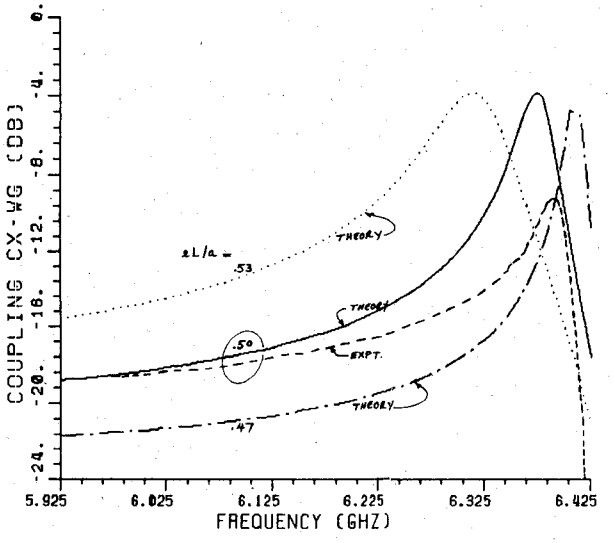

Fig. 5. Frequency response of coupling coefficient (S_{13}) in WR137 test model ($2W/b = 0.2$).

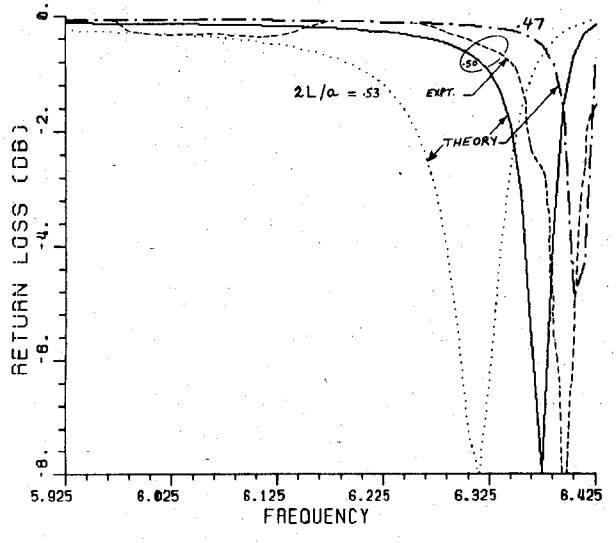

Fig. 6. Frequency response of return loss (S_{33}) in WR137 test model ($2W/b = 0.2$).

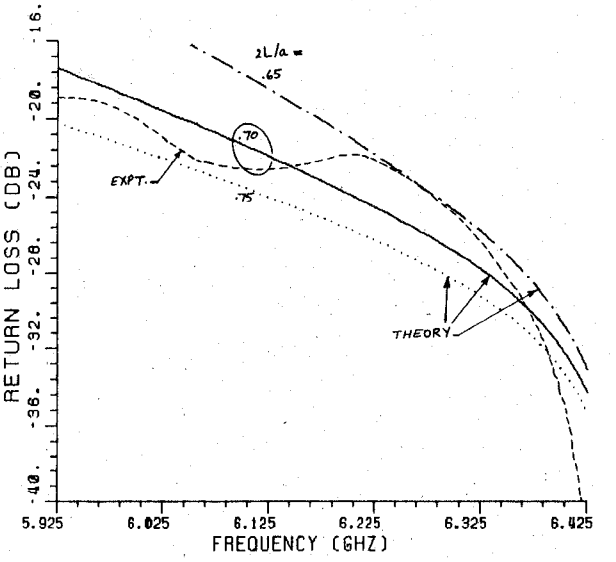

Fig. 7. Frequency response of return loss (S_{11}) in WR137 test model ($2W/b = 0.2$).

the slot reactance, given by (24), with the slot length and width. It is noted that, for the same coaxial guide, coupling into WR137 at 6.175 GHz presents a reactance that is more sensitive to slot dimensions and frequency compared to coupling into WR229 at 3.95 GHz. The higher slope of the X/Z_{11} curve in the former case means higher Q and narrower bandwidth. Likewise, within each frequency band, a wider slot results in a wider bandwidth.

Defining resonance as the case when $X = 0$, Fig. 4(a) tells us that, for the coaxial-to-WR137 junction, as the slot width increases the resonant length decreases. For the coaxial-to-WR229 junction, however, the resonant length increases as the slot width increases (Fig. 4(b)).

Figs. 5 and 6 give the frequency response of the coupling coefficient (S_{13}) and the return loss (S_{33}) of the coaxial-to-WR137 junction for slot length $2L/a = 0.47, 0.50, 0.53$. As expected, the slot resonance is associated with maximum coupling and minimum reflection in the rectangular waveguide.

D. Experimental Verification of the Theory

Comparisons between experimental and theoretical results are given in Figs. 5–7. In performing the experiment, the coaxial TE_{11} mode was launched by connecting port 1 to a coaxial-to-circular waveguide transition, then to a 2-port (WR137 and WR229) combiner connected to the test equipment. The experimental curves shown in Figs. 5–7 thus include contributions from those transitions, and that may explain why the measured coupling in Fig. 5 is lower than the theoretical curve, and why the measured return loss in Fig. 7 is fluctuating about the theoretical curve.

In all other respects, Figs. 5–7 show good agreement between theory and experiment especially if we were allowed to shift the theoretical curves of Figs. 5 and 6 toward the right. Such a small frequency shift may be attributed to the approximate nature of the variational approach which was employed in this analysis, or to the fact that the theory does not take into account the slot thickness. Quantitatively, the theoretical zero-thickness resonant length is approximately 3-percent shorter than the measured one (see Figs. 5 and 6). It is also noticeable (by comparing the width of the zero-thickness theoretical curve to the width of the experimental curve in Fig. 5) that the Q value for a zero-thickness slot is lower than that for a slot with finite thickness. Similar observations on the effect of slot thickness on the resonant length and Q were made by Oliner [8] in the case of a longitudinal radiating slot in a rectangular waveguide.

IV. Design Applications

According to the application, the primary design criterion for the subject T-junction may be selectively defined so as to maximize, minimize, or achieve a prescribed cou-

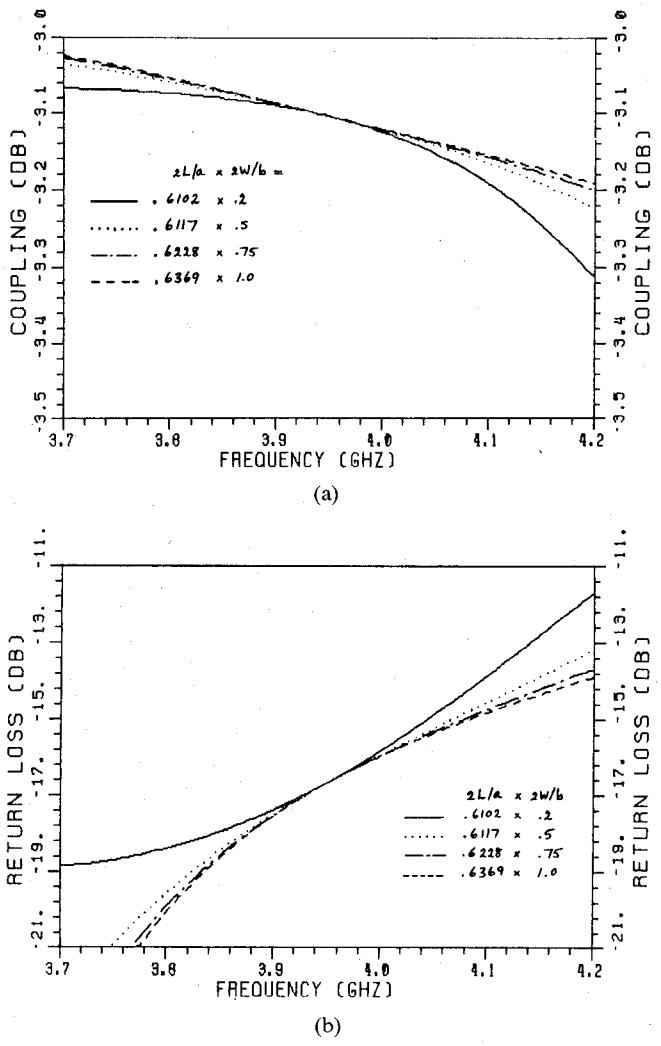

Fig. 8. Frequency response of the WR229 test model for four slots resonant at 3.95 GHz. (a) Coupling coefficient S_{13}. (b) Return loss S_{33}.

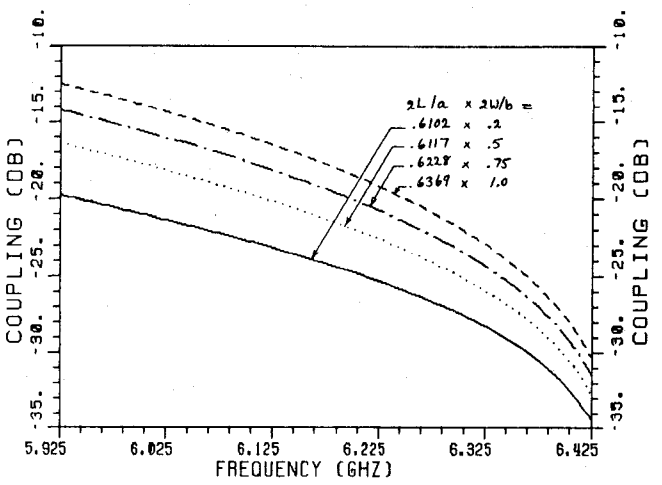

Fig. 9. Unwanted coupling (S_{13}) of a 6-GHz signal in the WR229 test model for four slots resonant at 3.95 GHz.

pling over a prescribed frequency band. These three cases are here discussed.

A. Maximum Coupling Applications

An example of such application is the 3-dB coupler. To maximize coupling, slot resonance has to be achieved usually at midband. Fig. 8 gives the frequency response of the coaxial-to-WR229 test model with four options of resonant slots. The optimum slot coupling is better than -3.2 dB and the return loss in WR229 is better than -14 dB across the band 3.7–4.2 GHz. The return loss can be reduced, of course, using tuning devices (e.g., screws) arranged in either or both the coaxial and rectangular waveguides. Reducing return loss will obviously increase coupling toward its -3-dB target.

If 0-dB coupling is required, the above design exercise still holds if complemented by a short-circuiting device located in the coaxial guide at an optimum distance from the slot. The device may be a transverse plate, an array of pins, or a band-reject filter.

B. Minimum Coupling Applications

In a coaxial diplexer, for example, coupling is to be maximized in one band and minimized in another. Fig. 9 shows the unwanted coupling through the same four resonant slots of Fig. 8 across the band 5.925–6.425 GHz. While a narrow slot is slightly less favorable for the desired coupling of the 4-GHz signal (see Fig. 8(a)), it is quite favorable to minimize the unwanted coupling of the 6-GHz signal (see Fig. 9). Again, the present design may be complemented by a 6-GHz filtering device inserted in WR229 so as to reject such undesirable coupling.

C. Prescribed Coupling Applications

An antenna array composed of rectangular waveguide radiators may be serially fed by a coaxial guide. The structure thus is composed of cascaded T-junctions with assigned coupling distribution. Having illustrated the slot coupling coefficient as arbitrarily chosen (Fig. 5), as maximized (Fig. 8(a)), and as minimized (Fig. 9), it is clear that utilizing the present theory to design each individual slot in the above array is a similarly achievable task. Further numerical examples would therefore be unnecessary.

V. Conclusions

The work reported in this paper comprises a theoretical analysis of the slot-coupled coaxial-to-rectangular waveguide T-junction, operating in the TE_{11} and TE_{10} modes, respectively. The validity of the analysis is proven experimentally. The characteristics of such a junction are illustrated by numerical examples. The power of the present analysis as a useful design tool is established through addressing specific design criteria and applications.

The approach of this paper can readily be utilized to solve the circular-to-rectangular waveguide T-junction which should yield simpler expressions considering the

simpler representation of circular waveguide eigenfunctions compared to those of a coaxial.

REFERENCES

[1] N. Marcuvitz, Ed., *Waveguide Handbook* (MIT Rad. Lab. Series, vol. 10). New York: McGraw-Hill, 1951.

[2] R. F. Harrington, *Time Harmonic Electromagnetic Fields*. New York: McGraw-Hill, 1961, ch. 7.

[3] N. Marcuvitz and J. Schwinger, "On the representation of the electric and magnetic fields produced by currents and discontinuities in waveguides," *J. Appl. Phys.*, vol. 22, no. 6, pp. 806–819, June 1951.

[4] G. Markov, *Antennas*. Moscow, USSR: Progress Publishers, 1965, ch. 7.

[5] B. N. Das, P. S. Deshmukh, and V. M. Pandharipande, "Excitation of planar slot array from rectangular waveguide," *Proc. Inst. Elec. Eng.*, vol. 131, pt. H, no. 2, pp. 99–101, Apr. 1984.

[6] V. M. Pandharipande and B. N. Das, "Equivalent circuit of a narrow-wall waveguide slot coupler," *IEEE Trans. Microwave Theory Tech.*, vol. MTT-27, pp. 800–804, Sept. 1979.

[7] C. G. Montgomery, R. H. Dicke, and E. M. Purcell, Eds., *Principles of Microwave Circuits* (MIT Rad. Lab. Series, vol. 8). New York: McGraw-Hill, 1948, sec. 12.15.

[8] A. A. Oliner, "The impedance properties of narrow radiating slots in the broad face of rectangular waveguide. Part II—Comparison with measurement," *IEEE Trans. Antennas Propagat.*, vol. AP-5, pp. 12–20, Jan. 1957.

Saad Michael Saad (M'77–SM'82) was born in Alexandria, Egypt, on February 11, 1945. He received the B.Sc. and M.Sc. degrees from Alexandria University, Egypt, in 1965 and 1969, respectively, and the Ph.D. degree from the University of London, England, in 1974, all in electrical engineering.

From 1965 to 1977, he was with the Electronics Research Institute of the National Research Center, Cairo, Egypt, except for the period 1970–1973, when he was with the Department of Electronic and Electrical Engineering of University College, London, England. During 1977–1978, he was a Research Associate at the Remote Sensing Laboratory of the University of Kansas. Since 1978, he has been with the Andrew Corporation, Orland Park, IL, where he is now Section Leader — Waveguide Components.

Dr. Saad's professional career has been devoted primarily to research and development in microwave passive components and antennas, with emphasis on numerical techniques and computer-aided design. He worked also as an Adjunct Assistant Professor at Ain Shams University (1975–1976) and the Military Technical College (1974–1976), both in Cairo, Egypt. He is now an Adjunct Associate Professor at the University of Illinois at Chicago.

Dr. Saad served as Secretary-Treasurer, Vice Chairman, and Chairman of the joint Chicago Chapter of the IEEE Antennas and Propagation Society and the Microwave Theory and Techniques Society (1981–1984). He is a Professional Engineer registered in the State of Illinois, holds several patents, and has authored and coauthored many technical publications.